Chinese Journal of Physics 96 (2025) 219–227

Contents lists available at ScienceDirect

Chinese Journal of Physics

journal homepage: www.sciencedirect.com/journal/chinese-journal-of-physics

Exploring the adsorption of 5-fluricil anticancer drug over the $Zn_{12}S_{12}$ nanostructure as a drug delivery system: DFT study

Umair Ahmed [a], Ali H. Reshak [b,c,d,*], Nada M. Abbass [e], Adnan Ali Khan [f,g], Sheraz Ahmad Khan [h], Ashif Sajjad [i], Muhammad Ayub [i], Dania Ali [j], Muhammad M. Ramli [d]

[a] Department of Chemistry, Balochistan University of Information Technology and Management Sciences, Quetta Balochistan, Pakistan
[b] Physics Department, College of Science, University of Basrah, Basrah 61004, Iraq
[c] Al-Kunooz University College, Basrah, Iraq
[d] Center of Excellence Geopolymer and Green Technology (CEGeoGTech), University Malaysia Perlis, 01007 Kangar, Perlis, Malaysia
[e] Department of Chemistry, College of Science, Baghdad University, Jaderiya, Baghdad, Iraq
[f] Centre for Computational Materials Science, University of Malakand, Chakdara, Pakistan
[g] Department of Chemistry, University of Malakand, Chakdara, Pakistan
[h] Department of Physics, Govt Dehgree College, Mingora Swat, Pakistan
[i] Institute of Biochemistry, University of Balochistan, Quetta Balochistan, Pakistan
[j] Faculty of medicine, Charles University, Pilsen 30100, Czech Republic

ARTICLE INFO

Keywords:
Drug delivery
5-fluorouracil
DFT
$Zn_{12}S_{12}$ nanocage
Adsorption energy

ABSTRACT

Applying density functional theory (DFT), the potential of zinc sulfide ($Zn_{12}S_{12}$) nanocage for delivery of 5-fluorouracil (5FU) is explored. Two stable adsorption modes are predicted for 5FU on $Zn_{12}S_{12}$. The basis set superposition error (BSSE) corrected adsorption energies of 5FU on a $Zn_{12}S_{12}$ are –14.70 and –13.50 kcal/mol for adsorption configuration-1 and 2, respectively. The results, on the other hand, show that up to 6 drug molecules can be attached on the surface of the $Zn_{12}S_{12}$ nanocage simultaneously, with –11.10 kcal/mol energy per 5FU molecule. Because of the moderate adsorption energies and charge-transfer values, the 5FU can be simply separated from the surface at ambient temperature. The 5FU may be easily protonated in the target cancerous tissues, which assists to release of the drug from nanocage. The 5FU adsorption energies decrease when solvent effect is applied. Results of this study validated the capability of pure $Zn_{12}S_{12}$ for delivery of multiple 5FU molecules.

1. Introduction

In the medical industry nanotechnology plays an essential role for the delivery of various drugs especially for the treatment of cancer [1]. To deliver anti-cancer drug to the affected parts of the body using various nanomaterials is a great challenge for the scientists in cancer therapy [2]. Therefore nano-structured drug carriers have achieved enormous improvements in intracellular diseases treatment [3–6]. Nanostructure drug delivery system modulate drug release characteristic, enhance drug solubility, reduce the side effects of drugs diminish drug toxicity and target drug molecules to the desired sites [7]. A lot of literature reported the

* Corresponding author.
E-mail address: maalidph@yahoo.co.uk (A.H. Reshak).

https://doi.org/10.1016/j.cjph.2025.01.034
Received 19 October 2024; Received in revised form 16 January 2025; Accepted 17 January 2025
Available online 17 January 2025

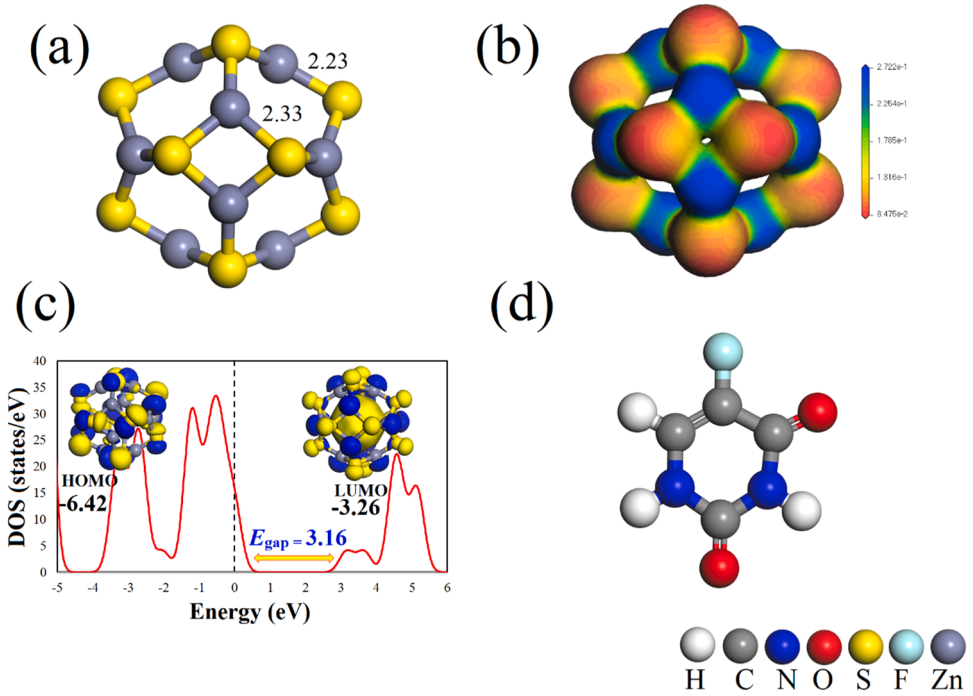

Fig. 1. (a) The optimized geometry of $Zn_{12}S_12$ nanocage, (b) corresponding molecular electrostatic potential map, (c) density of states plot, (d) and relaxed geometry of 5FU drug molecule.

nanostructures properties have been used as a promising targeted delivery of biological active agents into living systems i.e. carbon nanotubes [8], dendrimers [9], liposomes [10], polymer based [11], nanoshells [12], superparamagnetic and inorganic [13] materials. In various types of nanostructures, the allotropes of carbon including nanotubes, buckyballs and graphene have very significant applications in biotechnology and medical science due to is unique properties and structures [14,15]. Numerous literatures have been reported in which the properties of various carbon nanocage (fullerenes) is addressed for delivery of various anticancer drugs [16–18]. Therefore, the researchers have being redirected their great desire towards inorganic nanostructures as well and reported much literature about non-carbons nano-materials for drug delivery including boron-nitride (BN), silicon carbide (SiC), Magnesium oxide (MgO), zinc oxide (ZnO) and gallium nitride (GaN) theoretically [3,19–22]. Continued study of exploring properties of such nano-materials for various applications in drug delivery system, still of great interest and can add much to the body of knowledge.

The nanostructures belongs to II-VI semiconductors which have been reported extensively due to their remarkable properties and diverse applications [23]. Among the II-VI materials ZnO and ZnS are widely studied compounds. They are highly stable and aboundant evniormentally friendly nano-materials. Therefore, they are cooperative for bio-mdeical applications [24–26]. The $(ZnO)_{12}$ nanocluster used as a drug delivery vehchle in various studies [27,28] but $(ZnS)_{12}$ cluster not gain significant attention as a drug delvivery system especially for 5-fluricil (5FU) anticancer drug. 5FU is a fluorinated pyrimidine analog chemotherapeutic agent applying as solid cancer therapy like stomach, esophagus, carcinoma and intestines [29–32]. 5FU is interesting in pharmacology because it interferes with nucleoside metabolism via the competitive inhibition of thymidylate synthetase, the enzyme catalyzing the methylation of deoxyuridylic acid to thymidylic acid. Therefore, it inhibits DNA replication and repair and its depletion induces cytotoxicity and cell death [29–31,33].

Aim of present work is to investigate the adsorption of 5FU over the $Zn_{12}S_{12}$ nanostructures by employing density functional theory simulations. The main objectives of this work are, to study various geometrical interactions between 5FU and $Zn_{12}S_{12}$ nanostructure both in gas and solution phase, interaction energies and density of states of the formed complexes. Additionally the AIM analysis and NBO analyses were also performed to clearly understand the strength and nature of bonding between the 5FU drug and $Zn_{12}S_{12}$ nanostructure. We hope this study will help in future for designing of new nanomaterials consisting of ZnS atoms for drug delivery system.

2. Computational details

Computational calculations were performed using $DMol^3$ code [34]. The geometries were optimized using density functional theory (DFT) with the gradient corrected Perdew Burke Ernzernhof (PBE) exchange correction functional at the generalized-gradient-approximation (GGA) level [35]. A double-numerical with polarization functions (DNP) was used as a basis set. To compensate van der Waals interactions, the Grimme's scheme DFT-D2 method [36,37] was used. To perform an accurate computation, the geometry was optimized at 10^{-5} Ha convergence tolerances, 0.001 Ha/Å for the force and 0.005 Å for displacement.

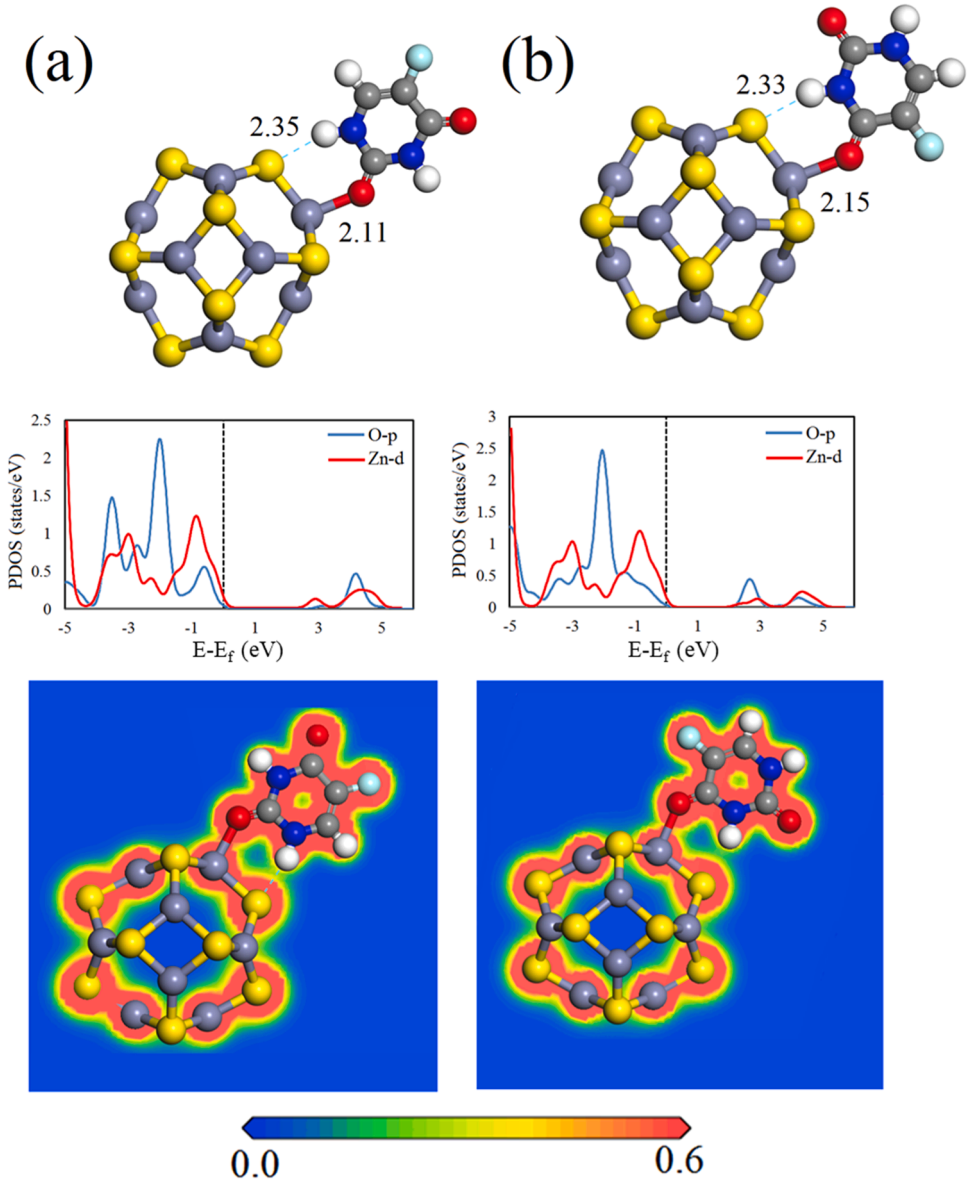

Fig. 2. The Optimized geometry of 5FU adsorption configuration-1 (a) and adsorption configuration-2 (b) over $Zn_{12}S_{12}$ nanocage and there corresponding partial density of states and electron density difference plots. Bond distance are in Å.

A Fermi smearing parameter of 0.005 Ha and 4.6 Å larger orbital cut-off was employed in the calculations. Frequency calculations were performed at STP using the same model chemistry to compute the thermochemistry as well as to verify that each optimized geometry corresponds to a minimum on the potential energy surface. Adsorption energies were evaluated as;

$$E_{ad} = E_{(Zn_{12}S_{12}+5FU)} - E_{(Zn_{12}S_{12})} - E_{(5FU)} - \delta\text{BSSE}\ , \tag{1}$$

where, $E_{(Zn12S12+5FU)}$ is the total energy of the ZnS nanocage and adsorbed drug molecule, $E_{(Zn12S12)}$ and $E_{(5FU)}$ is the energy of isolated ZnS nanocage and drug molecule. The E_{ad} were corrected for basis set superposition error (BSSE) by applying counterpoise correction [38]. The solvent effects were included by conductor-like screening model (COSMO) method [39]. The Multiwfn code [40] was used to obtained the atom in molecule results. The NBO program [41] was used for computations of second-order perturbation energy (E^2).

Table 1
Binding distance (Å), adsorption energy (E_{ad} kcal/mol), BSSE (kcal/mol), charge transfer (Q_{CT} e) and recovery time (τs) for 5FU adsorption over $Zn_{12}S_{12}$ nanocage in Ad-1 and Ad-2 in the gas phase.

Species	Zn—O	NH—S	E_{ad}	*BSSE*	E_{ad}+*BSSE*	Q_{CT}	τ
Ad-1	2.11	2.35	–16.49	1.79	–14.70	0.07, –0.06	0.0598
Ad-2	2.15	2.33	–14.81	1.31	–13.50	0.06, –0.05	0.0078
65FU@$Zn_{12}S_{12}$	2.12	2.14	–12.15	1.05	–11.10	0.06, –0.05	0.0001

*Positive value of charge transfer refer to donation while those with negative value refer to acceptance

3. Results and discussion

3.1. Gas phase optimized geometry of bare $Zn_{12}S_{12}$ nanostructure and isolated 5FU drug

The optimized geometry of $Zn_{12}S_{12}$ is depicted in Fig. 1. The $Zn_{12}S_{12}$ have nanocage like geometry which is previously reported [23, 42] resemble to the $(MgO)_{12}$, $(ZnO)_{12}$ and $(BN)_{12}$ nanocage having 6 tetragonal and 8 hexagonal rings. There are two types of bonding system in ZnS nanostructure i.e. S—Zn—S and Zn—S—Zn which joined by 4—6 and 6—6 membered ring system. The Zn—S bond length in 4—6 ring system is about 2.334 Å while in 6—6 ring system is about 2.227 Å. In both type of rings there are two types of angles formed among the atoms which are S-Zn-S and Zn-S-Zn. The S-Zn-S angle in both tetragonal and hexagonal ring has greater then Zn-S-Zn angle the values of angle S-Zn-S in hexagonal ring is roundabout 131.42^0 and Zn-S-Zn is 98.38^0 while in tetragonal ring is 96.58^0 and 76.35^0, respectively. The absence of imaginary frequency confirmed that the ZnS nanocage is a true minimum on the potential energy surface. These results are in good agreement with the previously reported results for $(ZnS)_{12}$ nanostructure.

To gain deeper insights into the drug adsorption over the ZnS nanostructure the surface analysis i.e. Mullikan population, Hirshfeld analysis and molecular electrostatic potential map (MEP) understanding is very significant for various configuration interaction of drug-nanostructure system. The Mullikan and Hirshfeld charge values indicated that the Zn atom has electropositive charge of 0.247 and 0.242 e while the S atom has electronegative charge of –0.255 and –0.250 e, respectively. The coloring MEP map (Fig. 1b) showing the electropositive and electronegative regions of nanostructure by blue and red color. The HOMO-LUMO gap and density of states for ZnS nanostructure computed by PBE is shown in Fig. 1c, which shows a semiconductor nature of the ZnS nanostructure having 3.16 eV energy gap (E_{gap}). The HOMO-LUMO profile is shown in Fig. 1 which clearly indicates that the HOMO is mostly contributed to S atom and the LUMO is contributed to Zn atom. To improve the energygap calculated by PBE, we used the PBE0 hybrid functional in the this study [43]. The energygap obtained at PBE0 hybrid funational is shown in Fig. S1, which is 3.07 eV. The formation energy for the $Zn_{12}S_{12}$ nanocage is calculated using the following equation;

$$E_f = [E_{(ZnS)n} - n \times E(ZnS)]/n \quad (2)$$

where, $E_{(ZnS)n}$ is the total energy of the ZnS nanocage and $E_{(ZnS)}$ is the energy of individual ZnS molecule. The formation energy for $Zn_{12}S_{12}$ nanocage is –2.87 eV/atom which is negative indicating the exothermic nature of nanocage and proofs the stability of the cage structure.

3.2. 5FU drug interaction with $Zn_{12}S_{12}$ nanostructure

The optimized geometries of different adsorption mode of 5FU drug over $Zn_{12}S_{12}$ nanocage are depicted in Fig. 2(a and b). We examined seven different adsorption modes, where the O, H and F site of 5FU drug interacted with Zn and S site of nanocage. The relaxed structures of the most stable complexes, there corresponding partial density of states (PDOS) and electron density difference (EDD) plots are represented in Fig. 2(a and b) while the other complexes (having weak interactions) are shown in Fig. S1. The optimized intermolecular bond lengths, adsorption energies and charge transfer values are given in Table 1. As illustrated in Fig. 2, two most table adsorption configuration for 5FU i.e. adsorption configuration-1, denoted by Ad-1 (where the carbonyl group in-between the two NH group of 5FU is directed towards the Zn atom and one H atom of NH group directed towards the S atom of nanocage) and adsorption configuration-2, denoted by Ad-2 (where the carbonyl group in neighbor of F atom of 5FU is directed towards the Zn atom and one H atom of NH group directed towards the S atom of nanocage). The geometry optimization reveals that two types of bonds appeared between the drug molecule and nanocage in both complexes i.e. Zn—O and NH—S bonds. The binding distance between the drug molecule and $Zn_{12}S_{12}$ nanocage is determined to be 2.11, 2.35, 2.15 and 2.33 Å for adsorption configuration-1 and 2, respectively. The BSSE corrected adsorption energy (E_{ad}) of 5FU is –14.70 and –13.50 kcal/mol on nanocage in Ad-1 and Ad-2, which falls within the range of chemisorption. The E_{ad} values of the 5FU molecule decrease as the drug molecule interacted from other sites as shown in Fig. S2, which is inconsistent with the degree of polarization and the Hirshfeld charge on these atoms. It should be noticed that the calculated E_{ad} values of the 5FU are more negative than those calculated on other surfaces such as $B_{24}N_{24}$ (–11.90 kcal/mol) [44] and Ge-doped BN nanotubes (–12.20 kcal/mol) [45]. The O atom of 5FU molecule serves as the electron donor in both optimized complexes, with a charge-transfer value of 0.07, and 0.06 electrons for adsorption Ad-1 and Ad-2, respectively. While the H atoms of 5FU act as acceptor, accepted 0.06 and 0.05 e from the nanocage surface. These findings clearly show that, in addition to electrostatic attraction between opposite charged atoms of 5FU and nanocage, orbital interactions also play an essential role in the formation of these complexes. In fact, the adsorption energies are well correlated with the amount of the charge transfer values between the 5FU

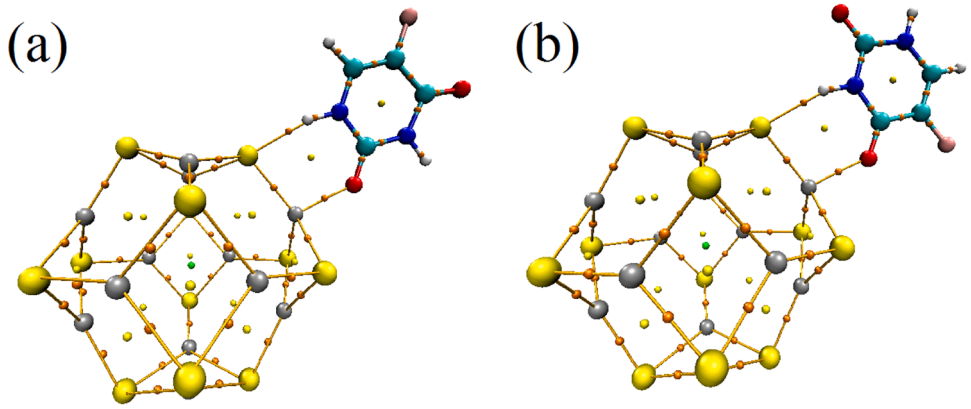

Fig. 3. Atom in molecule plots for Ad-1 (a) and Ad-2 (b). Gold small ball represent bond critical points and small yellow ball represent ring critical points.

Table 2
Atom in molecule parameter i.e. electron density (ρ au), Laplacian ($\nabla^2\rho$ au) energy density (H) and second order perturbation energy ($E^{(2)}$) for 5FU adsorption over $Zn_{12}S_{12}$ nanocage in Ad-1 and Ad-2.

	ρ		$\nabla^2\rho$		H		$E^{(2)}$	
Bonds	Zn—O	NH—S	Zn—O	NH—S	Zn—O	NH—S	Zn—O	NH—S
Ad-1	0.053	0.029	0.226	0.054	–0.009	–0.002	25.64	11.59
Ad-2	0.052	0.021	0.223	0.047	–0.007	–0.0003	25.07	6.24

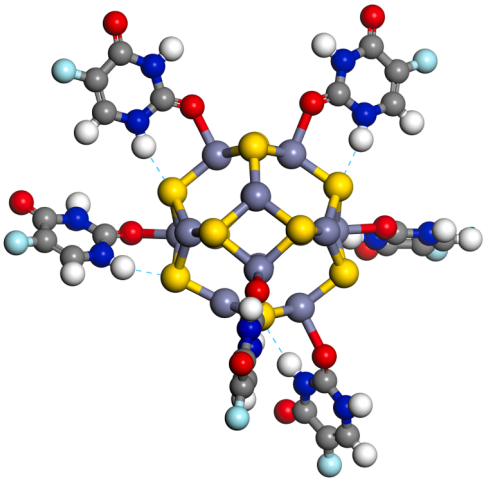

Fig. 4. Optimized geometry of 6 drug molecules adsorbed over the $Zn_{12}S_{12}$ nanocage.

and the $Zn_{12}S_{12}$ nanocage, suggesting that the charge-transfer is more essential for the stability of these complexes than the electrostatic interactions. This is confirmed further by the PDOS analysis, which shows that there is substantial overlap between the empty *d* orbital of the Zn atom and O-2*p* orbitals of the drug molecule around Fermi level. Note that compared to Ad-2, the degree of such orbital overlap is more important in Ad-1. To obtain more information about charge density distribution upon the adsorption of 5FU on nanocage, the EDD analysis is performed. As seen in Fig. 2, the adsorption of 5FU is associated with a considerable charge density rearrangement around the interacting atoms, suggesting that the mutual polarization of 5FU and $Zn_{12}S_{12}$ nanocage subunits upon the complex formation. In particular, the appearance of a large electron density loss region on Zn—O bonds of 5FU confirms that the atom serves as electron donor, which evidence the formation of stronger bond between the drug molecule and nanocage during the adsorption process. That is to say, the EDD analysis can be used as a suitable tool for assessing the adsorption strength between 5FU molecule and $Zn_{12}S_{12}$ nanocage. Compared to the previous reported studies [46,47] the 5FU molecule adsorption over $Zn_{12}S_{12}$ shows similar interactions i.e chemisorption nature and adsorption energies are almost in similar range. Moreover, the C=O site interacted chemically with the surface as interacted with Au_{32} nanocage [46].

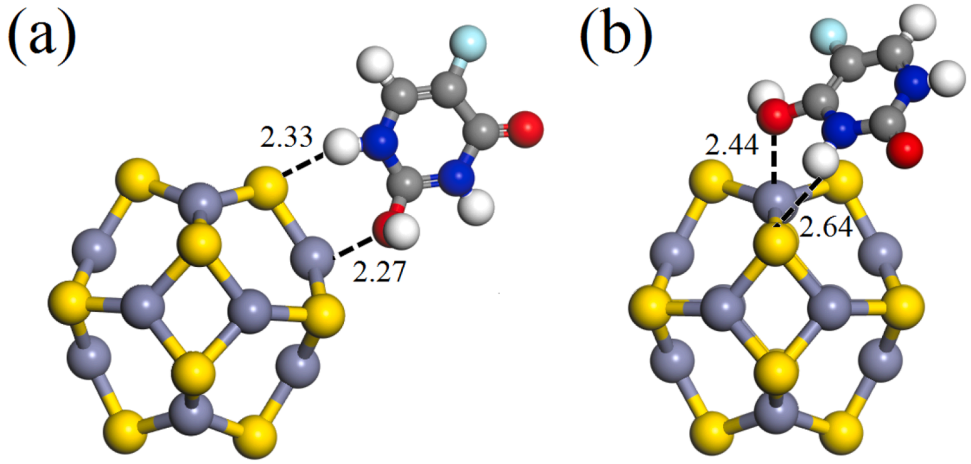

Fig. 5. The optimized geometry of protonated 5FU adsorption on $Zn_{12}S_{12}$ nanocage Ad-1 (a) and Ad-2 (b).

Atom in molecule (AIM) and natural bonding orbital analyses were performed to gain deeper insights into the strength of interactions between 5FU molecule and $Zn_{12}S_{12}$ nanocage. The AIM plots are illustrated in Fig. 3(a and b), which confirm that there is stronger intermolecular interactions exist between the 5FU drug and nanocage. The electron density (ρ) and Laplacian ($\nabla^2\rho$) values (Table 2) are fall in the range of strong intermolecular bonds [48,49]. The larger Laplacian values (Table 2) for both types of bonds i.e. Zn—O and NH—S in both complexes while the negative value of total energy density (H) indicating that the adsorption of 5FU drug is mainly driven by electrostatic effects [48,49]. This is further justified by the values of second-order perturbation energy (E^2) values summarized in Table 2. The E^2 value for LP(O)→LP*(Zn) charge transfer for Zn—O bond in Ad-1 is 25.64 kcal/mol while for LP(S)→σ*(HN) in S—HN bond is 11.59 kcal/mol. Similarly in Ad-2 the E^2 value for LP(O)→LP*(Zn) in Zn—O bond is 25.07 kcal/mol and for LP(S)→σ*(HN) in S—HN bond is 6.24 kcal/mol, respectively. The results of NBO analysis are in good agreement with the structural, energetic, charge transfer and AIM analysis, which shows that in both complexes the 5FU drug adsorbed over the $Zn_{12}S_{12}$ via two stronger bonds i.e. Zn—O and NH—S bonds.

The above information, indicates that the bare $Zn_{12}S_{12}$ surface can strongly adsorbed the 5FU drug molecule. Therefore, we also explored the maximum drug loading capacity of the nanocage system. We placed a 5FU molecule on each Zn-S bond and relaxed the resulting complexes. Fig. 4 illustrates the optimized structure of the derived complex, and Table 1 lists the adsorption energies and charge-transfer values. The calculated BSSE corrected adsorption energies per 5FU are –11.10 kcal/mol, indicating that the Zn and S atoms in this system can efficiently adsorb 5FU molecules. Due to repulsion effects between the adsorbed 5FU molecules, these average E_{ad} value are slightly lower than the E_{ad} value of the single 5FU drug adsorption. While the binding distances (Zn—O and NH—S bonds) are almost similar to the single 5FU molecule adsorption.

3.3. Drug release

For the effective drug release on target site, stable adsorption of drug molecules on the carrier surface is necessary. However, physisorption of drug on the carrier surface is considered best, because it does not cause desorption issues on the targe site. The adsorption energies of –13.50 kcal/mol and –14.70 kcal/mol are observed for the two most stable orientations of 5FU over $Zn_{12}S_{12}$ nanocage. The adsorption energy results of 5FU@$Zn_{12}S_{12}$ nanocage are in the physisorption range. This reveals that $Zn_{12}S_{12}$ nanocage may effectively desorb 5FU drug on target site. The adsorption strength of 5FU drug can easily be affected by a slight increase in temperature because cancer cells are slightly at a high temperature compared to the rest of the body cells. This effect of temperature and desorption of 5FU drug is carried out by the transition theory equation [50–52]:

$$\tau = \nu^{-1}\exp\left(\frac{E_{ads}}{k_B T}\right). \tag{3}$$

Here, τ is the desorption time of the drug from the cage, ν is the frequency (10^{12} Hz), T for temperature, k_B is the Boltzmann constant and E_{ad} is the adsorption energy of the drug molecule. The desorption time of 0.0078 and 0.059 sec is observed for 5FU from nanocage (see Table 1). The calculated time is short enough for 5FU drug release from nanocage

The 5FU delivery to cancerous cells is also carried out by the pH effect. The pH level of cancerous cells is usually less than 7 [53]. This shows that when 5FU molecules react with H+ at cancer cell. To observe this effect, we did the geometry optimization of 5FU@nanocage in the presence of a proton. The computed results show that proton is coupled on highly electronegative oxygen ends of 5FU drug molecule, which decreases the adsorption strength of 5FU with nanocage atoms (Fig. 5). After protonation, a decrease in adsorption energies for configurations 1(–10.65 kcal/mol) and 2 (–10.07 kcal/mol) are noticed compared to a neutral complex of 5FU@nanocage. The decrease in adsorption energy reveals the increase in interaction distance and enhancement of drug desorption from nanocage.

Table 3
Calculated adsorption energies (E_{ad}, kcal/mol), charge-transfer (Q_{CT}, |e|) and desorption times (τ, s) of adsorbed 5FU molecule on $Zn_{12}S_{12}$ nanocage in the aqueous phase.

Species	E_{solv}	E_{ad}	Q_{CT}	τ
Ad-1	–24.53	–14.13	0.06, –0.04	0.022
Ad-2	–21.68	–12.01	0.05, –0.04	0.0006

3.4. Solvent effects

The solubility and stability of 5FU@ $Zn_{12}S_{12}$ complexes in an aqueous medium are predicted through the solvation energy effect. The solvation energies of both configurations are calculated by taking the difference of energies of complexes in gaseous as well as in aqueous medium. In addition to solvation energy, charge transfer between 5FU and nanocage is calculated in an aqueous medium to analyze the solvation effects. The studied values of adsorption, solvation, charge transfer, and desorption time are presented in Table 3. Negative sing of solvation energies pointed to the stability of 5FU@ $Zn_{12}S_{12}$ nanocage complex in an aqueous medium. The adsorption energy values resulting in solvation effects are relatively smaller than in the aqueous phase due to the interaction of water molecules with drug molecules in an aqueous medium. Similarly, a slight decrease in charge transfer happened between drug and nanocage in an aqueous medium due to an increase in interacting distance. The incorporation of solvation energies in Eq. 3 can reduce the desorption time 5FU drug from $Zn_{12}S_{12}$. It is concluded from studied results that, 5FU can easily be desorbed from $Zn_{12}S_{12}$ nanocage in an aqueous medium compared to the gaseous phase.

4. Conclusions

In this study, a Grime's dispersion corrected DFT exploration of the ability of bare zinc sulfide ($Zn_{12}S_{12}$) nanocage was conducted. It was found that the Zn and S atom are the active sites on the hexagon rings of $Zn_{12}S_{12}$ nanocage and the nanocage can function as active nanostructure for the delivery of 5FU drug molecules. The 5FU drug molecule interacted via its O and H site strongly with the exterior surface of nanocage. This is confirmed by electron density difference, atom in molecule and natural bonding orbital analysis. Our findings indicated that bare $Zn_{12}S_{12}$ nanocage can carry up to 6 drug molecules with a binding energy of –11.10 kcal/mol. The protonated 5FU molecule E_{ad} values is significantly lower than those for a un-protonated 5FU, signifying that the 5FU-drug molecules can be easily separated from the nanocage when it reaches to the targeted cells. The inclusion of solvent environment decreases the strength of drug nanocage complexes, proposing that the 5FU release process is assisted by solvent system. This study validated for the first-time that how the bare zinc sulfide nanocage may significantly adsorbed the 5FU drug molecule and the total capacity of this system for carrying many 5FU drug molecules.

CRediT authorship contribution statement

Umair Ahmed: Data curation. **Ali H. Reshak:** Writing – review & editing. **Nada M. Abbass:** Data curation. **Adnan Ali Khan:** Formal analysis. **Sheraz Ahmad Khan:** Methodology. **Ashif Sajjad:** Software. **Muhammad Ayub:** Investigation. **Dania Ali:** Methodology. **Muhammad M. Ramli:** Data curation.

Declaration of competing interest

The authors declare that they have no known competing financial interests or personal relationships that could have appeared to influence the work reported in this paper.

Supplementary materials

Supplementary material associated with this article can be found, in the online version, at doi:10.1016/j.cjph.2025.01.034.

References

[1] M. Kurban, İ. Muz, Theoretical investigation of the adsorption behaviors of fluorouracil as an anticancer drug on pristine and B-, Al-, Ga-doped C36 nanotube, J. Mol. Liq. 309 (2020), https://doi.org/10.1016/j.molliq.2020.113209.
[2] M.K. Hazrati, N.L. Hadipour, Adsorption behavior of 5-fluorouracil on pristine, B-, Si-, and Al-doped C_{60} fullerenes: a first-principles study, Phys. Lett. Sect. A: Gener. Atom. Solid State Phys. 380 (2016), https://doi.org/10.1016/j.physleta.2016.01.020.
[3] I. Ravaei, M. Haghighat, S.M. Azami, A DFT, AIM and NBO study of isoniazid drug delivery by MgO nanocage, Appl. Surf. Sci. 469 (2019), https://doi.org/10.1016/j.apsusc.2018.11.005.
[4] Y. Namiki, T. Fuchigami, N. Tada, R. Kawamura, S. Matsunuma, Y. Kitamoto, M. Nakagawa, Nanomedicine for cancer: lipid-based nanostructures for drug delivery and monitoring, Acc. Chem. Res. 44 (2011), https://doi.org/10.1021/ar200011r.
[5] R.G. Mendes, A. Bachmatiuk, B. Büchner, G. Cuniberti, M.H. Rümmeli, Carbon nanostructures as multi-functional drug delivery platforms, J. Mater. Chem. B (2013) 1, https://doi.org/10.1039/c2tb00085g.

[6] N.R. Soman, G.M. Lanza, J.M. Heuser, P.H. Schlesinger, S.A. Wickline, Synthesis and characterization of stable fluorocarbon nanostructures as drug delivery vehicles for cytolytic peptides, Nano Lett. 8 (2008), https://doi.org/10.1021/nl073290r.
[7] M. Vatanparast, Z. Shariatinia, Computational studies on the doped graphene quantum dots as potential carriers in drug delivery systems for isoniazid drug, Struct. Chem. 29 (2018), https://doi.org/10.1007/s11224-018-1129-x.
[8] A. Bianco, K. Kostarelos, M. Prato, Applications of carbon nanotubes in drug delivery, Curr. Opin. Chem. Biol. 9 (2005), https://doi.org/10.1016/j.cbpa.2005.10.005.
[9] V. Brunetti, L.M. Bouchet, M.C. Strumia, Nanoparticle-cored dendrimers: functional hybrid nanocomposites as a new platform for drug delivery systems, Nanoscale 7 (2015), https://doi.org/10.1039/c4nr04438j.
[10] B.S. Pattni, V.V. Chupin, V.P. Torchilin, New developments in liposomal drug delivery, Chem. Rev. 115 (2015), https://doi.org/10.1021/acs.chemrev.5b00046.
[11] Y. Fazli, Z. Shariatinia, Controlled release of cefazolin sodium antibiotic drug from electrospun chitosan-polyethylene oxide nanofibrous Mats, Mater. Sci. Eng. C (2017) 71, https://doi.org/10.1016/j.msec.2016.10.048.
[12] B. Kumar, K. Jalodia, P. Kumar, H.K. Gautam, Recent advances in nanoparticle-mediated drug delivery, J. Drug. Deliv. Sci. Technol. 41 (2017), https://doi.org/10.1016/j.jddst.2017.07.019.
[13] C.S. Kim, G.Y. Tonga, D. Solfiell, V.M. Rotello, Inorganic nanosystems for therapeutic delivery: Status and prospects, Adv. Drug. Deliv. Rev. 65 (2013), https://doi.org/10.1016/j.addr.2012.08.011.
[14] S. Marchesan, M. Prato, Nanomaterials for (Nano)medicine, ACS Med. Chem. Lett. 4 (2013), https://doi.org/10.1021/ml3003742.
[15] D. Iannazzo, A. Pistone, M. Salamò, S. Galvagno, R. Romeo, S.V. Giofré, C. Branca, G. Visalli, A. Di Pietro, Graphene quantum dots for cancer targeted drug delivery, Int. J. Pharm. 518 (2017), https://doi.org/10.1016/j.ijpharm.2016.12.060.
[16] B.T. Tomić, C.S. Abraham, S. Pelemiš, S.J. Armaković, S. Armaković, Fullerene C_{24} as a potential carrier of ephedrine drug-a computational study of interactions and influence of temperature, Phys. Chem. Chem. Phys. 21 (2019), https://doi.org/10.1039/c9cp04534a.
[17] A. Hosseinian, E. Vessally, S. Yahyaei, L. Edjlali, A. Bekhradnia, A density functional theory study on the interaction between 5-fluorouracil drug and C24 fullerene, J. Clust. Sci. 28 (2017), https://doi.org/10.1007/s10876-017-1253-6.
[18] S. Bashiri, E. Vessally, A. Bekhradnia, A. Hosseinian, L. Edjlali, Utility of extrinsic [60]fullerenes as work function type sensors for amphetamine drug detection: DFT studies, Vacuum (2017) 136, https://doi.org/10.1016/j.vacuum.2016.12.003.
[19] D. Farmanzadeh, M. Keyhanian, Computational assessment on the interaction of amantadine drug with $B_{12}N_{12}$ and $Zn_{12}O_{12}$ nanocages and improvement in adsorption behaviors by impurity Al doping, Theor. Chem. Acc. 138 (2019), https://doi.org/10.1007/s00214-018-2400-3.
[20] N. Wazzan, K.A. Soliman, W.S.A. Halim, Theoretical study of gallium nitride nanocage as a carrier for 5-fluorouracil anticancer drug, J. Mol. Model. 25 (2019), https://doi.org/10.1007/s00894-019-4147-8.
[21] R. Padash, A. Sobhani-Nasab, M. Rahimi-Nasrabadi, M. Mirmotahari, H. Ehrlich, A.S. Rad, M. Peyravi, Is it possible to use $X_{12}Y_{12}$ (X = Al, B, and Y = N, P) nanocages for drug-delivery systems? A DFT study on the adsorption property of 4-aminopyridine drug, in: Appl. Phys. A Mater. Sci. Process., 124, 2018, https://doi.org/10.1007/s00339-018-1965-y.
[22] Y. Shen, Y. Shen, L. Zhang, C. Shi, M. Eslami, A computational study on the thioguanine drug interaction with silicon carbide graphyne-like nanosheets, Monatsh. Chem. 151 (2020), https://doi.org/10.1007/s00706-020-02706-2.
[23] W. Zhu, X.Q. Liu, X. Hou, J. Chen, C.K. Kim, K. Xu, Modelling of catalytically oxidative decomposition of carbon tetrachloride on a ZnS nanocluster using density functional theory, Catal. Sci. Technol. 4 (2014), https://doi.org/10.1039/c3cy00916e.
[24] F. Niederdraenk, K. Seufert, P. Luczak, S.K. Kulkarni, C. Chory, R.B. Neder, C. Kumpf, Structure of small II-VI semiconductor nanoparticles: a new approach based on powder diffraction, Phys. Status Solid. (C) Curr. Top. Solid State Phys. 4 (2007), https://doi.org/10.1002/pssc.200775423.
[25] J.M. Azpiroz, E. Mosconi, F. De Angelis, Modeling ZnS and ZnO nanostructures: Structural, electronic, and optical properties, J. Phys. Chem. C (2011) 115, https://doi.org/10.1021/jp2083709.
[26] E. Jimenez-Izal, I. Ortiz De Luzuriaga, E. Ramos-Cordoba, J.M. Matxain, Role of Dispersion Interactions in Endohedral TM@(ZnS)12Structures, ACS Omega, 2021, https://doi.org/10.1021/acsomega.1c02016.
[27] X. Ji, S. Jameh-Bozorghi, Metal oxide nanoclusters as drug delivery systems for an anticancer drug: a theoretical study, Mol. Phys. 118 (2020), https://doi.org/10.1080/00268976.2020.1738581.
[28] H. Li, M.R.P. Heravi, A.G. Ebadi, S. Ahmadi, A. Sarkar, Study the nature of the interaction between 5-fluorouracil anti-cancer drug and zinc oxide nanocage, Braz. J. Phys. 52 (2022), https://doi.org/10.1007/s13538-022-01062-2.
[29] J.D. Sara, J. Kaur, R. Khodadadi, M. Rehman, R. Lobo, S. Chakrabarti, J. Herrmann, A. Lerman, A. Grothey, 5-fluorouracil and cardiotoxicity: a review, Ther. Adv. Med. Oncol. 10 (2018), https://doi.org/10.1177/1758835918780140.
[30] K.R. Stefaniak, C.C. Epley, J.J. Novak, M.L. McAndrew, H.D. Cornell, J. Zhu, D.K. McDaniel, J.L. Davis, I.C. Allen, A.J. Morris, T.Z. Grove, Photo-triggered release of 5-fluorouracil from a MOF drug delivery vehicle, Chem. Commun. 54 (2018), https://doi.org/10.1039/c8cc01601a.
[31] P. Lvarez, J.A. Marchal, H. Boulaiz, E. Carrillo, C. Vélez, F. Rodrguez-Serrano, C. Melguizo, J. Prados, R. Madeddu, A. Aranega, 5-fluorouracil derivatives: a patent review, Exp. Opin. Ther. Pat. 22 (2012), https://doi.org/10.1517/13543776.2012.661413.
[32] G.J. Ogunwale, H. Louis, T.O. Unimuke, G.E. Mathias, A.E. Owen, H.O. Edet, O.C. Enudi, E.O. Oluwasanmi, A.S. Adeyinka, M.D. Mohammadi, Interaction of 5-fluorouracil on the surfaces of pristine and functionalized $Ca_{12}O_{12}$ nanocages: an intuition from DFT, ACS Omega 8 (2023), https://doi.org/10.1021/acsomega.2c03635.
[33] E. Carrillo, S.A. Navarro, A. Ramírez, M.Á. García, C. Griñán-Lisón, M. Perán, J.A. Marchal, 5-fluorouracil derivatives: a patent review (2012 - 2014), Exp. Opin. Ther. Pat. 25 (2015), https://doi.org/10.1517/13543776.2015.1056736.
[34] B. Delley, An all-electron numerical method for solving the local density functional for polyatomic molecules, J. Chem. Phys. 92 (1990) 508–517, https://doi.org/10.1063/1.458452.
[35] J.P. Perdew, K. Burke, M. Ernzerhof, Generalized gradient approximation made simple, Phys. Rev. Lett. 77 (1996) 3865–3868, https://doi.org/10.1103/PhysRevLett.77.3865.
[36] S. Grimme, Accurate description of van der Waals complexes by density functional theory including empirical corrections, J. Comput. Chem. 25 (2004) 1463–1473, https://doi.org/10.1002/jcc.20078.
[37] S. Grimme, Semiempirical GGA-type density functional constructed with a long-range dispersion correction, J. Comput. Chem. 27 (2006) 1787–1799, https://doi.org/10.1002/jcc.20495.
[38] A. Rahmanzadeh, M. Rezvani, M. Darvish Ganji, M. Tale Moghim, Corrosion protection performance of Laurhydrazide N′-propan-3-one (LHP) adsorbed on zinc surface: A DFT-MD simulation investigation, Mater. Today Commun. 36 (2023) 106946, https://doi.org/10.1016/j.mtcomm.2023.106946.
[39] A. Klamt, G. Schüürmann, COSMO: a new approach to dielectric screening in solvents with explicit expressions for the screening energy and its gradient, J. Chem. Soc. 2 (1993), https://doi.org/10.1039/P29930000799. Perkin Transactions.
[40] T. Lu, F. Chen, Multiwfn: a multifunctional wavefunction analyzer, J. Comput. Chem. 33 (2012) 580–592.
[41] A.E. Reed, L.A. Curtiss, F. Weinhold, Intermolecular Interactions from a natural bond orbital, donor—acceptor viewpoint, Chem. Rev. 88 (1988), https://doi.org/10.1021/cr00088a005.
[42] S. Hamad, C.R.A. Catlow, E. Spano, J.M. Matxain, J.M. Ugalde, Structure and properties of ZnS nanoclusters, J. Phys. Chem. B 109 (2005) 2703–2709.
[43] M. Mohammadzaheri, S. Jamehbozorgi, M.D. Ganji, M. Rezvani, Z. Javanshir, Toward functionalization of ZnO nanotubes and monolayers with 5-aminolevulinic acid drugs as possible nanocarriers for drug delivery: a DFT based molecular dynamic simulation, Phys. Chem. Chem. Phys. 25 (2023) 21492–21508, https://doi.org/10.1039/D3CP01490H.
[44] M.K. Hazrati, Z. Javanshir, Z. Bagheri, B24N24 fullerene as a carrier for 5-fluorouracil anti-cancer drug delivery: DFT studies, J. Mol. Graph. Model. 77 (2017), https://doi.org/10.1016/j.jmgm.2017.08.003.
[45] A. Soltani, M.T. Baei, E. Tazikeh Lemeski, S. Kaveh, H. Balakheyli, A DFT study of 5-fluorouracil adsorption on the pure and doped BN nanotubes, J. Phys. Chem. Solid. 86 (2015), https://doi.org/10.1016/j.jpcs.2015.06.008.

[46] M. Sabet, S. Tanreh, A. Khosravi, M. Astaraki, M. Rezvani, M.D. Ganji, Theoretical assessment of the solvent effect on the functionalization of Au_{32} and C_{60} nanocages with fluorouracil drug, Diam. Relat. Mater. 126 (2022) 109142, https://doi.org/10.1016/j.diamond.2022.109142.
[47] M.D. Ganji, M. Mohseni, O. Goli, Modeling complexes of NH_3 molecules confined in C_{60} fullerene, J. Molecul. Struct.: THEOCHEM 913 (2009) 54–57, https://doi.org/10.1016/j.theochem.2009.07.015.
[48] A. Ali Khan, M.D. Esrafili, R. Ahmad, I. Ahmad, Al-decorated $C_{24}N_{24}$ fullerene: a robust single-atom catalyst for CO oxidation, Polyhedron 210 (2021) 115497, https://doi.org/10.1016/j.poly.2021.115497.
[49] I. Rozas, I. Alkorta, J. Elguero, Behavior of ylides containing N, O, and C atoms as hydrogen bond acceptors, J. Am. Chem. Soc. 122 (2000) 11154–11161.
[50] A.A. Khan, R. Ahmad, I. Ahmad, Density functional theory study of emerging pollutants removal from water by covalent triazine based framework, J. Mol. Liq. 309 (2020) 113008, https://doi.org/10.1016/j.molliq.2020.113008.
[51] J. Prasongkit, R.G. Amorim, S. Chakraborty, R. Ahuja, R.H. Scheicher, V. Amornkitbamrung, Highly sensitive and selective gas detection based on silicene, J. Phys. Chem. C (2015) 119, https://doi.org/10.1021/acs.jpcc.5b03635.
[52] L. Kou, T. Frauenheim, C. Chen, Phosphorene as a superior gas sensor: Selective adsorption and distinct i - V response, J. Phys. Chem. Lett. 5 (2014), https://doi.org/10.1021/jz501188k.
[53] G. Hao, Z.P. Xu, L. Li, Manipulating extracellular tumour pH: an effective target for cancer therapy, RSC Adv. 8 (2018), https://doi.org/10.1039/c8ra02095g.